Geologic and Topographic Features of Slope Failure Sites in the Aso Caldera Wall Induced by the 2016 Kumamoto Earthquake

Haruka SAITOU[1*], Shin'ya KATSURA[2], Ryota UMETANI[1],
Mio KASAI[2] and Tomomi MARUTANI[2]

[1] Graduate School of Agriculture, Hokkaido University, Japan
[2] Research Faculty of Agriculture, Hokkaido University, Japan
[*]Corresponding author. E-mail: daifuku.oneone@gmail.com

INTRODUCTION

A large-scale earthquake with an epicenter in the Kumamoto Prefecture, Kyushu Region, Japan, occurred on 16 April 2016 (the 2016 Kumamoto earthquake). The Kumamoto earthquake had a maximum seismic intensity of 7 on the Japan Meteorological Agency (JMA) seven-stage seismic scale and a JMA magnitude of 7.3. Aso Caldera is a large caldera in the Kumamoto Prefecture measuring about 17 km in the east–west direction and about 25 km north to south, formed by a catastrophic eruption 270,000 to 90,000 years ago. A seismic intensity of 6 lower on the JMA seven-stage seismic scale was registered in the Aso Caldera area during the 2016 Kumamoto earthquake, which resulted in numerous slope failures and extensive damage.

To implement countermeasures to mitigate damage from slope failures effectively, it is necessary to identify locations where the possibility of slope failure is high.

The purpose of this study was to clarify the geologic and topographic features of slope-failure sites in the wall of Aso Caldera caused by the 2016 Kumamoto earthquake.

STUDY AREA

The study area was in the northwestern part of the Aso Caldera wall, Kumamoto Prefecture (22.1 km^2; **Fig. 1**). The geology of the Aso Caldera wall consists of pyroclastic flow deposits, including welted tuff formed by catastrophic eruptions about 270,000 to 90,000 years ago (called Aso-1 to 4), andesite older than Aso-1 to 4, and talus accumulations (formed by the accumulation of rock debris) roughly from the top to the bottom. The area and average slope of each geology are shown in **Tab. 1**. In this area, light detection and ranging (LiDAR) data were obtained in 2012 (before the earthquake) and in 2016 (after the earthquake).

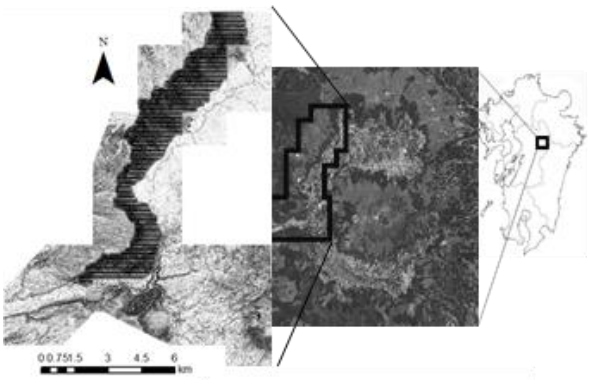

Fig. 1 Study area

GEOLOGIC AND TOPOGRAPHIC ANALYSES

We compared the elevation on a 1-m digital elevation model (DEM) prepared from 2016 data with 2012 LiDAR data and classified areas that showed negative change in elevation as a slope failure site. The identified slope failure sites were confirmed by aerial photographs acquired after

the earthquake. We investigated the elevation, slope, and curvature (an index representing the unevenness of the terrain: positive and negative values indicate convex and concave shapes, respectively) of the slope failure sites using a 10-m DEM prepared from 2012 LiDAR data. These values were calculated for each mesh using a geographic information system (GIS). Then, the values of a slope failure site were calculated by averaging the values of all meshes overlapping all or part of the slope failure site. The geology of each slope failure site was investigated using the Aso Volcano geologic map (Ono and Watanabe, 1985).

RESULTS AND DISCUSSION

The slope failure density (number of slope failures per unit area) is shown in **Tab. 1**. The slope failure density was largest for pyroclastic flow deposits, suggesting that slope failures occurred most densely in these deposits. The probable reasons that the pyroclastic flow deposits showed a larger slope failure density than the andesite or talus accumulation are that 1) pyroclastic flow deposits formed more recently and are therefore geologically weak and 2) the average slope is steeper in the pyroclastic flow deposits than in the talus accumulation (**Tab. 1**).

Table 1 Area, average slope, and slope failure density for each geology

Geology	Area (km^2)	Average slope (degree)	Slope failure density (/km^2)
Pyroclastic flow deposits	3.2	31.4	18.4
Andesite	10.1	31.3	12.0
Talus accumulation	7.4	14.5	0.5

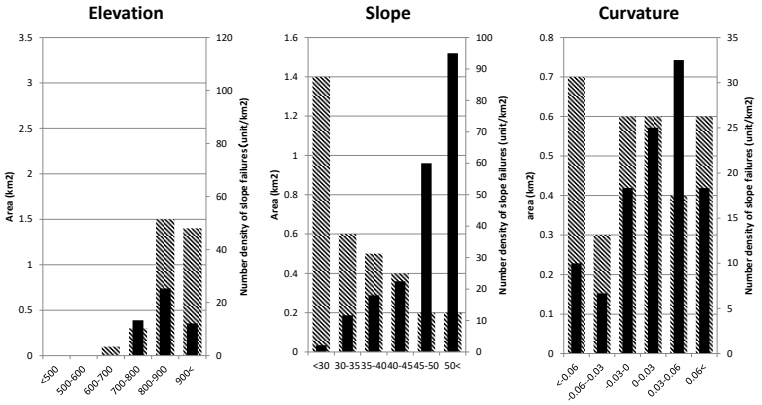

Fig. 2 Slope failure density for each class of elevation, slope, and curvature in the pyroclastic flow deposits

The slope failure density for each class of elevation, slope, and curvature was calculated for the pyroclastic flow deposits, which showed the largest slope failure density, as shown in **Fig. 2**. The slope failure density was large for high elevations (>700 m) and positive curvature (convex shape) and also increased with increasing slope. These results suggest that slope failures are more likely to occur at slopes that are more unstable when affected by intense shaking, as shown in previous studies (e.g., Nishida *et al.*, 1996).

CONCLUSION

This study analyzed the geologic and topographic features of slope failure sites in the wall of Aso Caldera resulting from the 2016 Kumamoto earthquake. In future work, it would be desirable to develop further the method of evaluating slope failure risk by a large-scale earthquake for individual slopes.

REFERENCES: Ono and Watanabe (1985), Geological Map of Aso Volcano, Geological Survey of Japan; Nishida *et al*. (1996), Journal of the JSECE, Vol. 49, No.1, p. 19–24

ACKNOWEDGEMENTS: This study was supported by the Ministry of Land, Infrastructure, Transport and Tourism (MLIT), Japan. The LiDAR data were provided by the Kyushu Regional Development Bureau, MLIT.

Keywords: 2016 Kumamoto Earthquake, Aso Caldera wall, geology, slope failure, topography